

## Carbon Footprint Tracking and Quantitative Analysis Model for Power Industry Based on Thermodynamics



Wei Hu\*, Xue Xia

School of Economics and Management, Shanghai University of Electric Power, Shanghai 200090, China

Corresponding Author Email: [hwshiep@shiep.edu.cn](mailto:hwshiep@shiep.edu.cn)

<https://doi.org/10.18280/ijht.400507>

### ABSTRACT

**Received:** 10 June 2022

**Accepted:** 28 August 2022

#### Keywords:

*carbon inventory, carbon footprint, carbon exergy ratio, thermodynamics, thermal map*

Since the concept of carbon asset is still new to most power enterprises, they generally lack the knowledge and experience of carbon asset management, to help them cope with the related works, this paper proposes a carbon footprint tracking and quantitative analysis model for power enterprises based on thermodynamics. At first, by employing thermodynamic theories, this paper established an inventory model through the measurement and calculation of carbon concentration and carbon emissions, which can fix defective items, improve inventory efficiency, and save inventory cost. Then, the paper used thermo-economics and the TOPSIS method to construct a carbon inventory index system containing indexes such as carbon exergy ratio and regulation interval, which can reduce the error of carbon emission intensity and update the carbon account information in a timely manner. After that, the carbon footprint was calculated by coupling the carbon thermal map with the multi-dimensional evaluation mechanism, thereby achieving accurate control of carbon emissions and realizing the energy-saving and emission-reduction goals. At last, the attained experimental results showed that, the proposed carbon inventory measurement model established based on thermodynamics can effectively regulate the emission behavior of power enterprises, help achieve the ultimate purposes of reducing cost, increasing efficiency, and optimizing environment. The work done in this paper could provide theoretical support for making decisions for the smooth development of carbon rights market in China.

## 1. INTRODUCTION

Huge amount of greenhouse gases (GHGs) could be produced during production and transportation processes, leading to a series of environmental problems such as global warming, species decline, and rise in sea level, etc., which have seriously damaged the ecosystems we human race rely for existence [1, 2]. The key factor behind global warming is the emission of GHGs, such as CO<sub>2</sub>, O<sub>3</sub>, CH<sub>4</sub>, and N<sub>2</sub>O, etc. [3], among these gases, CO<sub>2</sub> is regarded as the most dangerous and pervasive GHG due to its significant role in global warming. Therefore, tracking the carbon footprint of high-emission areas is very meaningful for achieving the goals of peak carbon emissions and carbon neutrality.

World field scholars have attained fruitful research results in many aspects in the carbon field. For instance, Babar et al. [4] performed data envelope analysis (DEA) on carbon permits market and simulated the energy and carbon trading in different scenarios, the authors took carbon market as a policy tool to study green growth factors and achieve the goals of energy conservation and emission reduction. Fenner et al. [5] introduced the many advantages of carbon rights trading market in terms of improving market liquidity, lowering carbon rights trading price, and reducing carbon emissions of power enterprises. The paper analyzed the influencing factors of carbon rights trading policies on the carbon emission performance of cities, creating a low-carbon and healthy environment for carbon rights trading. Lenze et al. [6]

introduced that China has opened the carbon rights trading market since 2011, after that, seven pilot projects of carbon rights trading market have been organized, and it's found during the work of these projects that the low-carbon transformation could be achieved through the carbon price mechanism. These studies explored the application of carbon market from different angles but there isn't one that builds quantitative analysis model by coupling carbon footprint tracking system with thermodynamic theories.

Thermodynamics is a branch of physics that studies the transformation of energy from the perspective of macroscopic changes and development of systems [7]. Basic laws of thermodynamics include the first and the second laws, wherein the second law of thermodynamics is the core content of this subject [8]. Achievements in thermodynamics can affect not only the natural sciences, but also social sciences and philosophy. Modern thermodynamics and classical thermodynamics together constitute the complete discipline of thermodynamics [9]. In recent years, the description and manipulation of carbon footprint tracing using quantitative analysis based on thermodynamic theories have received more attention from field scholars.

Based on above concerns, this paper proposed a quantitative analysis model for carbon footprint tracing of power industry based on thermodynamics. At first, this paper employed thermodynamic theories to construct a complete carbon inventory model that can rapidly fix high-emission items and effectively control the inventory cost. Then, through the model

of thermo-economics, five first-level indexes were set to improve the accuracy of carbon emission intensity, and the regulatory agency set caps of carbon emissions to reward and punish the carbon emission behavior of power enterprises. At last, thermal maps were plotted and a multi-dimensional carbon footprint assessment mechanism was established to lower the carbon emissions and realize the 3060 low-carbon goal.

## 2. THEORETICAL BASIS

### 2.1 Basic theories of thermodynamics

For a carbon inventory system, its thermodynamic state can be described by external variables such as temperature  $T$ , strain  $\varepsilon$ , temperature gradient  $\nabla T$ , and a series of internal state variables. Under the action of external load, the state variables would change constantly with the microstructure inside the carbon inventory system. It is generally believed that the energy dissipation during this process is irreversible, and it should conform to the first and second laws of thermodynamics [10, 11].

Expression of the first law of thermodynamics (the law of conservation of energy) in the form of rate is:

$$\rho \dot{e} - \sigma : \dot{\varepsilon} + \nabla \cdot q - \rho \gamma = 0 \quad (1)$$

where,  $\rho$  represents the inventory density;  $e = \varphi + Ts$  is the specific internal energy, wherein  $\varphi$  represents the Helmholtz free energy,  $s$  represents the specific entropy, and  $T$  represents the temperature;  $\sigma$  is the tensor of stress;  $\dot{\varepsilon}$  is the differential of strain tensor  $\varepsilon$  with respect to time  $t$ ;  $q$  represents the heat flux density vector;  $\gamma$  represents the specific heat supply rate;  $\nabla$  represents the gradient operator.

Expression of the second law of thermodynamics (the principle of entropy increase) in the form of rate is:

$$\rho T \dot{s} + \nabla \cdot q - \frac{q}{T} \cdot \nabla T - \rho \gamma \geq 0 \quad (2)$$

### 2.2 Assessment model of thermo-economics

Thermo-economic indexes can measure the energy-saving potential of power plants, they include the standard coal consumption rate of power generation and the power generation efficiency of the entire plant, wherein the standard coal consumption rate of power generation  $l_m$  is:

$$l_m = 3600 / (Q_{net} \mu_b \mu_p \mu_e) \quad (3)$$

where,  $Q_{net}$  represents the lower heating value of standard coal and its value takes 29270kJ/kg;  $\mu_b$  represents the efficiency of boiler and its value takes 94%;  $\mu_p$  represents the efficiency of pipeline and its value takes 99%;  $\mu_e$  represents the absolute electric efficiency of the steam turbine generator set,  $\mu_e = 3600/q_0$ , wherein  $q_0$  is the heat consumption rate, then the power generation efficiency of the entire plant is:

$$\mu_t = \frac{1000W_t A}{l_m Q_{net}} \quad (4)$$

where,  $W_t$  is the power of electricity generation;  $A$  is the

electric heat, and it takes 3600  $kJ(kw \cdot h)$ .

## 3. CARBON INVENTORY CALCULATION

This paper introduced the internal damage variable, and coupled it with the viscoelastic deformation to describe the Helmholtz free energy  $\varphi = \varphi^{ve}(\varepsilon^{ve}, D)$  [12]. Based on the basic theories of thermodynamics, the carbon concentration and carbon emissions were calculated respectively.

### 3.1 Calculation of carbon concentration

In the past two decades, the burning of large amounts of coal, oil and gas of the industrial sector and the deforestation are main reasons for the increase of carbon dioxide concentration in the atmosphere [13, 14]. This paper improved the calculation method of Chen and Millero (MCM) [15] and measured the produced or consumed dissolved inorganic carbon (DIC) through biological process ( $C^{bio}$ ) inventory. The measured DIC includes the natural carbon ( $C^{O.PT}$ ) and the artificial carbon ( $C^{ant}$ ), therefore, the calculation method of artificial carbon concentration is:

$$C^{ant} = DIC - C^{bio} - C^{O.PT} \quad (5)$$

$$C^{bio} = 0.5 \times \Delta TA - (C/O_2 + 0.5N/O_2) \cdot \Delta O_2 \quad (6)$$

$$\Delta TA = TA - TA^0 \quad (7)$$

$$\Delta O_2 = O_2^0 - O_2^{mes} \quad (8)$$

where,  $TA$  and  $TA^0$  respectively represent the measured and the pre-formed basicity;  $C/O_2$  and  $N/O_2$  are the molar ratios proposed by Anderson based on the average composition of the planktonic organics ( $C:N:P:-O_2=106:16:1:-150$ );  $O_2^{mes}$  and  $O_2^0$  are respectively the measured and the preformed concentrations of dissolved oxygen;  $\Delta O_2$  represents oxygen consumption;  $\theta$  represents the ratio of potential temperature;  $S_p$  represents the practical salinity. Then, through the inventory of surface area (0-150m), it can be calculated that:

$$TA^0 = 93.779S_p - 0.57\theta - 1004.765 (\pm 7.5 \mu mol / kg) \quad (9)$$

### 3.2 Calculation of carbon emissions

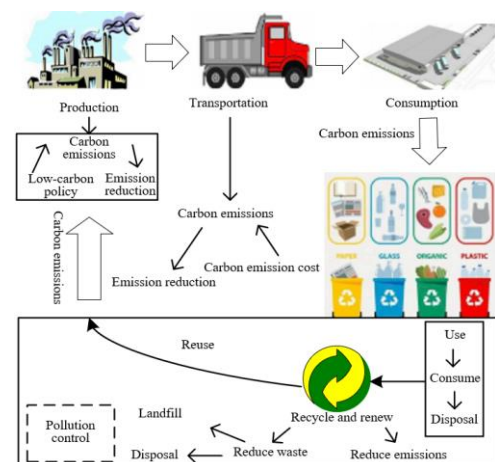


Figure 1. Diagram of carbon emissions

According to the IPCC theory, this paper classified the calculation of carbon emissions into the energy part, the industrial part, and the solid waste part [16], as shown in Figure 1.

$$(1) \text{ Energy part: } Q_e = \sum_k \left( \frac{44}{12} \times 10^{-4} \cdot h_k \cdot cq_k \cdot cv_k \right)$$

$Q_e$  represents the total amount of GHG emissions generated by the production or consumption of various types of energy;  $44/12$  is the ratio of carbon dioxide to the carbon element;  $10^{-4}$  is the unit conversion coefficient;  $h_k$  is the release amount of fuel  $k$ ;  $cq_k$  is the carbon content of the fuel  $k$  for per unit calorific value;  $cv_k$  is the carbon oxidation rate contained in fuel  $k$ .

$$(2) \text{ Industrial part: } Q_l = q_k \cdot \bar{y}_k \cdot l_k$$

$Q_l$  represents the total amount of GHG emissions generated from industrial processes other than fuel combustion;  $q_k$  represents the output of industrial product  $k$ ;  $\bar{y}_k$  represents the average emission factor of product  $k$  during the industrial production process;  $l_k$  represents the carbon conversion coefficient of the different types of industrial product  $k$ .

$$(3) \text{ Solid waste part: } Q_c = \sum \left( \frac{44}{12} \times j \cdot \chi \cdot \kappa \cdot p \right)$$

$Q_c$  represents the amount of CO<sub>2</sub> emissions produced from the incineration of solid wastes;  $j$  represents the amount of processed incinerated solid wastes;  $\chi$  represents the proportion of carbon element in the solid wastes;  $\kappa$  represents the proportion of carbon element in various minerals in the total amount of carbon element in the treated substance;  $p$  represents the efficiency of the solid waste treatment equipment.

## 4. CARBON INVENTORY SYSTEM BASED ON THERMODYNAMICS

### 4.1 The carbon inventory model based on carbon thermal map

In order to realize the orderly storage and quick query of the data of carbon thermal maps, it is necessary to encode the map tile data and shorten the distance between the data in the same area and their physical storage positions [17]. They are saved as blanks, see Table 1.

**Table 1.** Data storage mode of carbon thermal map

Row Key	Time stamp	IMAGE			
		XY1	XY2	XY3	XY4
Key1	T1	IMAGE1	IMAGE2	IMAGE3	IMAGE4
Key2	T2	IMAGE15	IMAGE6	—	—
Key3	T3	IMAGE7	IMAGE8	—	—

In this paper, the thermal maps were plotted based on the Web GIS visualization technology of the DBSCAN clustering architecture. When loading the thermal map, the Web browser will number the map tiles according to the area and send request to the server, the server end takes the tile number as the query condition to determine the map data. After that, the server end returns the attained map data to the Web end, and the Web end will calculate the grayscale value according to the count value of the clustering results and plot the thermal map. Image data of different levels and different areas are stored in different data tables, and the coding method is shown in Figure 2. The columns are named using the tile numbers. During each

query, map data can be searched according to the X and Y numbers of the tiles.

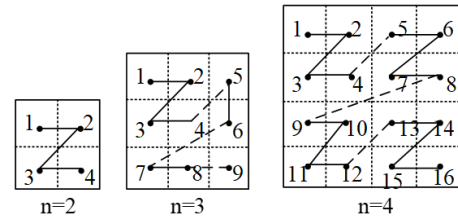


**Figure 2.** Coding method of carbon thermal map

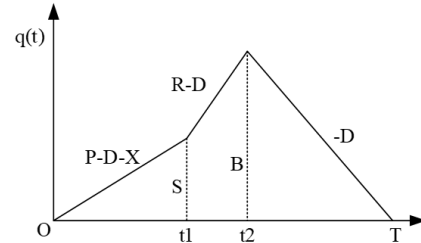


**Figure 3.** The change of carbon inventory level with time

In China, the current carbon inventory system is not standardized [18], so this paper designed a novel inventory model based on carbon thermal map according to the characteristics of different time periods, which can effectively control the inventory cost and improve the inventory efficiency. It's set that the inventory cycle starts from  $t=0$ , the inventory speed is  $P$ ; under a demand rate  $D$  the regular inventory lasts until  $t=t_1$ . Due to inevitable factors, some defective items are examined at a speed of  $X$ , the net inventory accumulation rate is  $P-D-X$  during this period, and the inventory level reaches  $S$  at  $t=t_1$ . Defective items need to be re-examined so that they can be perfectly repaired with speed  $R$ , and the repair process lasts until  $t=t_2$ . Assuming: the inventory level reaches  $B$  at  $t=t_2$ , after that, the inventory level is consumed out due to the demand of the client end, and it reaches 0 at  $t=T$ . The entire scenario is shown in Figure 3 and can be described by the following differential equations:

$$\frac{dq(t)}{dt} = \begin{cases} P - X - D & 0 \leq t \leq t_1 \\ R - D & t_1 \leq t \leq t_2 \\ -D & t_2 \leq t \leq T \end{cases} \quad (10)$$

It should meet these conditions  $q(0)=0$ ,  $q(t_1)=S$ ,  $q(t_2)=B$ , and  $q(T)=0$ . By replacing the values of  $D$  and  $X$ , we can get:

$$\frac{dq}{dt} = \begin{cases} P(1-\alpha) - \alpha + bp & 0 \leq t \leq t_1 \\ R - \alpha + bp & t_1 \leq t \leq t_2 \\ -\alpha + bp & t_2 \leq t \leq T \end{cases} \quad (11)$$

Moreover, it should meet these conditions  $q(0)=0$ ,  $q(t_1)=S$ ,  $q(t_2)=B$ , and  $q(T)=0$  as well. Under given conditions, the above differential equations could be solved:

$$q(t) = \begin{cases} Pt \cdot (1-\alpha) - \alpha t + bpt & 0 \leq t \leq t_1 \\ R(t-t_1) - (\alpha - bp)t + P(1-\alpha)t_1 & t_1 \leq t \leq t_2 \\ (\alpha - bp)(T-t) & t_2 \leq t \leq T \end{cases} \quad (12)$$

At this time, the boundary condition of the defective items is  $y(0)=0$ , and the inventory level is:

$$\begin{aligned} \frac{dy(t)}{dt} &= X; 0 \leq t \leq t_1 \\ \Rightarrow \frac{dy(t)}{dt} &= P\alpha; 0 \leq t \leq t_1 \end{aligned} \quad (13)$$

By solving the above differential equations, we have  $y(t)=Pat$ ;  $0 \leq t \leq t_1$ . Since the unit of the defective item  $Q\alpha$  has been repaired at a speed of  $R$  within time interval  $[t_1, t_2]$ , we have:

$$R(t_2 - t_1) = Q \quad (14)$$

According to the continuity of Formula 8, at  $t = t_2 = t_1 + \frac{Q\alpha}{R}$ , it can be deduced that:

$$T = \frac{R(t_2 - t_1) + P(1 - \alpha)t_1}{\alpha - bp} \quad (15)$$

In this cyclic system, the inventory batch number  $Q$  is:

$$Q = \int_0^{t_1} P dt = Pt_1 \quad (16)$$

Next, the various inventory costs related to the inventory cycle are assessed. Since the composition of the various inventory costs is the interval number, the different costs involved in inventory are also interval numbers.

As previously mentioned, carbon emissions are mainly derived from the construction process, manufacturing process, reprocessing process, and inventory process. Next, the costs related to the inventory cycle are assessed. Since the composition of the various inventory costs is the interval number, the different costs involved in inventory are also the interval numbers. Here, it's set that the cost of carbon emissions within the inventory cycle is  $\bar{e}_s = [e_{sL}, e_{sR}]$ ; the cost of carbon emissions during inventory multiplied by the batch number  $Q$  is  $\bar{e}_p = [e_{pL}Pt_1, e_{pR}Pt_1]$ , and the cost of carbon emissions held during inventory multiplied by the inventory area is:

$$\bar{e}_h = [e_{hL}, e_{hR}] \left[ \begin{array}{l} P(1 - \alpha)(t_1t_2 - \frac{t_1^2}{2}) + \frac{R}{2}(t_2 - t_1)^2 \\ + (\alpha - bp)(\frac{T^2}{2} - Tt_2) \end{array} \right] \quad (17)$$

Similarly, the cost of carbon emissions during inventory review multiplied by the number of repair items is  $\bar{e}_r = [e_{rL}\alpha Pt_1, e_{rR}\alpha Pt_1]$ . Therefore, the total amount of carbon emissions during one inventory cycle is also an interval value given by  $\overline{CE} = [CE_L, CE_R]$ .

$$\begin{aligned} CE_L &= e_{sL} + e_{pL}Pt_1 \\ &+ e_{hL} \cdot [P(1 - \alpha)(t_1t_2 - \frac{t_1^2}{2}) + \frac{R}{2}(t_2 - t_1)^2 \\ &+ (a - bp)(\frac{T^2}{2} - Tt_2)] + e_{rL}\alpha Pt_1 \end{aligned} \quad (18)$$

$$\begin{aligned} CE_R &= e_{sR} + e_{pR}Pt_1 \\ &+ e_{hR} \cdot [P(1 - \alpha)(t_1t_2 - \frac{t_1^2}{2}) + \frac{R}{2}(t_2 - t_1)^2 \\ &+ (a - bp)(\frac{T^2}{2} - Tt_2)] + e_{rR}\alpha Pt_1 \end{aligned} \quad (19)$$

## 4.2 Carbon inventory index system based on thermal economics

There are certain errors with the calculation of carbon emission intensity of the power industry in China, and the inventory accounts of the power industry are hysteretic [19]. Therefore, this paper employed the thermodynamic theories and the TOPSIS method to construct carbon exergy ratio, input/output ratio, environmental variables, and regulatory index  $\lambda$  to adjust the relationship between carbon inventory and energy saving and emission reduction.

Thermal economics defines the input and output streams of the equipment to be the "fuel" and the "product" respectively.  $F$  is the exergy of fuel,  $P$  is the exergy of product,  $u$  is the exergy loss. Then the exergy balance equation is  $F=P+u$ .

Theorem 1: Carbon emission intensity is the ratio of carbon emissions to total GDP.

Theorem 2: Exergy efficiency  $\xi=P/F$  measures the ratio of exergy gain to exergy loss of a certain stage or a certain equipment during the carbon inventory process, and its value is between  $[0, 1]$ .

(1) Carbon exergy ratio: It measures the relationship between carbon emissions and exergy loss during the inventory process, and it is an index related to energy conservation and emission reduction during inventory. The exergy efficiency is positively related to the effect of energy conservation and emission reduction. This paper set two kinds of carbon exergy ratio indexes, one is the carbon exergy process ratio  $\varepsilon$  which is used to analyze the exergy loss for per unit carbon emissions during the inventory; smaller value of  $\varepsilon$  indicates that the carbon is more prone to be completely neutralized during the inventory process or be converted into other energy forms and released. The other is the carbon exergy efficiency  $\eta$  which is used to analyze the exergy efficiency for per unit carbon emissions during the inventory; greater value of  $\eta$  indicates that a higher exergy efficiency is achieved with less carbon emissions during the inventory. These two indexes should be analyzed together, only using  $\varepsilon$  or  $\eta$  can mislead the works of energy conservation and emission reduction, thereby causing errors and deviations to the carbon emission intensity of power enterprises.

$$\varepsilon = \frac{u_t}{CE_t} \quad (20)$$

$$\eta = \frac{\xi}{v_t} \quad (21)$$

where,  $u_t$  is the exergy loss vector within period  $t$  during the inventory;  $CE_t$  is the carbon dioxide emission within period  $t$  during the inventory;  $v_t$  is the ratio of the carbon contents at the inlet and outlet within period  $t$  during the inventory, namely the carbon emission efficiency. When the values of  $\varepsilon$  and  $\eta$  are close, it indicates that the emission of GHGs is large; if the values of the two are equal, it indicates that the carbon burnt has been completely released; if the values of the two are

very different, it indicates that the carbon in the raw materials has been retained during the inventory, and the inventory of this project should be reviewed.

(2) Regulatory index  $\lambda$ : regulatory agency imposes fines or taxes on projects with a per unit carbon emission that exceeds the standards during the inventory process; moreover, in order to encourage enterprises whose emissions are lower than the fixed cap, it will reward enterprises with a per unit carbon emission that is lower than the fixed cap.

Considering that  $\lambda=[\lambda_L, \lambda_R]$  is an interval number, the total tax will be an interval number as well. In this case, when the carbon emission of an enterprise is lower than the fixed cap, it can sell the remaining tax permits to other enterprises. Assuming:  $\beta=[\beta_L, \beta_R]$  is the unit inventory index, when its value is positive, it represents reward; when its value is negative, it represents punishment. Within an inventory cycle, the attained total regulatory index  $[\lambda_L, \lambda_R]$  is:

$$\lambda_L = (C \cdot T - CE_R) \times \beta_L \quad (22)$$

$$\lambda_R = (C \cdot T - CE_L) \times \beta_R \quad (23)$$

To make enterprises strictly comply to the policy of a carbon emission lower than cap  $C$ , the regulatory index  $\lambda$  must be imposed on the total amount of carbon emissions within the

inventory cycle, and the cap is:

$$CE_R \leq C \cdot T \quad (24)$$

(3) Input index: for the input of carbon inventory of electricity power, three second-level indexes that are related to the measurement and calculation have been selected, namely capital, energy, and labor consumption. The existing power enterprise carbon inventory models generally lack the capital index. The input capital of the power industry carbon inventory is represented by the investment amount of fixed assets; in addition, the second-level index labor consumption is represented by the number of employees at year end of the power industry carbon inventory; and the second-level index energy is represented by the consumption amount of natural gas, coal gangue, raw coal, and other energy sources.

(4) Output index: for the output of carbon inventory of electricity power, this paper set desired output (production value of generated electricity) and undesired output (carbon emissions). After the factor of inflation has been eliminated from the desired output, the measurement and calculation of the carbon inventory of power industry can be represented by the sales value of the industry in previous years; the second-level index undesired output is represented by the measured value of carbides (Table 2).

**Table 2.** Description of input-output indexes

Variable	Unit	Max	Min	Mean	Standard deviation	Range
Capital	100 million yuan	1705.54	6.18	301.20	262.47	1699.35
Energy	10000 tons of standard coal	14638.85	83.38	3142.40	593	14555.47
Labor	100 people	3320	120	1087.78	2832.21	3100
Production value of generated electricity	100 million yuan	6641.39	15.26	854.61	1027.56	6626.13
Carbon emissions	10000 tons	28723.17	164.917	6163.40	5538.20	28558.26

(5) Environmental variables: according to the different research objects and emphases of carbon inventory, this paper selected economic level and environmental regulation as the environmental variables. The comprehensive development capability of the power industry is determined by the economic level. The economic development of power enterprise carbon inventory is represented by the per capita GDP. The environmental level is related to the intensity of environmental regulation, and the environmental regulation of carbon inventory is represented by the proportion of investment of pollution control in the GDP [18].

### 4.3 Multi-dimensional carbon footprint assessment mechanism

In terms of carbon footprint measurement, this paper proposed a multi-dimensional dynamic assessment system based on carbon thermal map, the system contains four low-carbon subsystems: economy, management, control, and environment, and it can effectively control carbon emissions in various dimensions. In a complete life cycle of the power industry, carbon emissions mainly form carbon footprints during energy transportation, storage, retail and trade processes.

Theorem 3: carbon footprint refers to the amount of carbon emissions directly or indirectly caused by human behaviors such as production and consumption.

(1) Carbon footprint of energy storage of power industry.

$$C_{store} = NT \cdot D \cdot \sum_{i=1}^m P_i \cdot E \cdot \mu \quad (25)$$

where,  $NT$  is the quantity of energy inventory,  $D$  is the average number of days of energy consumption of electricity customers,  $P_i$  is the daily energy consumption of electricity customer  $i$ ;  $E$  is the carbon emission intensity of energy transmission;  $\mu$  is the carbon emission conversion factor.

(2) Carbon footprint of energy interaction.

The carbon footprint of energy interaction mainly refers to the energy consumption in the power industry during the process of power generation. The calculation formula is as follows:

$$C_{tran} = \sum_{i=1}^m \sum_{j=1}^n G_i \cdot H_j \cdot \beta_j \quad (26)$$

where,  $C_{tran}$  represents the interactive carbon footprint;  $G_i$  is the purchased amount of electricity customer  $i$ ;  $H_j$  is the energy consumption of electricity customer  $i$ .

(3) Carbon footprint of solid wastes.

The carbon footprint of solid waste in the power industry is divided into the methane emissions from solid waste landfills and the carbon emissions from solid waste treatment. The former is based on IPCC and can be calculated as follows:

$$C_{CH_4} = s \cdot \eta \cdot DOC \cdot \omega \cdot (16/12) \cdot 0.5 \frac{1}{1000} \quad (27)$$

where,  $C_{CH_4}$  is the methane emissions generated from the landfills;  $s$  is the quantity of garbage in the landfill, its unit is kilograms;  $\eta$  represents the landfill rate;  $DOC$  is the amount of biodegradable organic carbon in the solid wastes;  $\omega$  represents the decomposition rate of biodegradable organic carbon, referring to IPCC, its value takes 77%. The carbon footprint of energy consumption of solid waste treatment is:

$$C_{CO_2} = s \cdot \eta \cdot \sum_{j=1}^n E_j \cdot \beta_j \quad (28)$$

where,  $E_j$  is the energy consumption of the treatment of per kilogram solid waste;  $\beta_j$  is the carbon emission coefficient of energy  $j$ . The carbon footprint of solid wastes in the power industry is:

$$C_{solidwast} = C_{CH_4} \cdot GEP_{CH_4} + C_{CO_2} \quad (29)$$

where,  $GEP_{CH_4}$  is the global warming energy of methane relative to carbon dioxide.

#### (4) Carbon footprint of green energy

Afforestation, energy conservation, and emission reduction are effective ways to achieve carbon neutrality, but if plants are damaged by human or natural disasters, or their development space has been inhibited, their ability of carbon absorption will be weakened. The formula for calculating carbon emission capacity is:

$$NPP_{destroy} = \sum_{j=1}^n \frac{A_j^2 \cdot \alpha_j}{A} \quad (30)$$

where,  $NPP_{destroy}$  is the destroyed carbon absorption ability of the plants;  $j$  is the land utilization type;  $\alpha_j$  is the carbon emission coefficient of land  $j$ ;  $A_j$  is the area of land  $j$ ;  $A$  is the total area.

## 5. EXAMPLE ANALYSIS

### 5.1 Carbon thermal map loading test

To examine the rendering efficiency of thermal maps based on clustered data, in this study, visual test was performed on clustered data with scale levels of 11, 12, 13, and 14, respectively, and the results are shown in Figure 4.

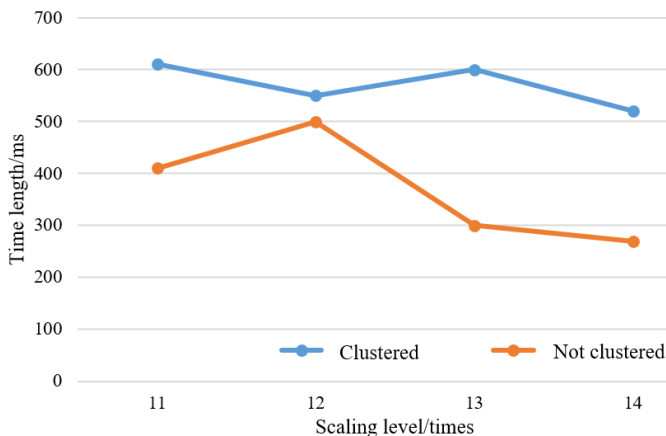


Figure 4. Time length comparison of data loading

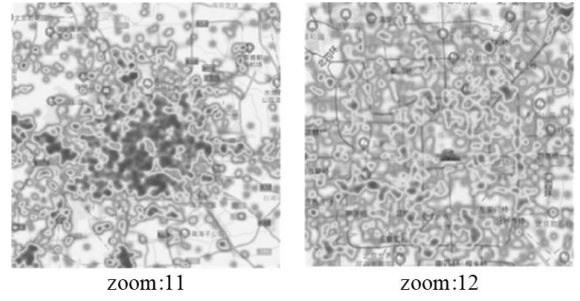


Figure 5. Visualization effect

As the scale level increases, the generation time of thermal maps shows a trend of shortening; when the scale level is relatively low, for the original data and the processed data, the difference in the visualization time is very small; but when the scale level is relatively high, the generation time of visual map of the processed data decreases significantly, and when moving or scaling the maps, there's no obvious frame hysteresis. After scaling, thermal maps are generated, as shown in Figure 5, which has proved the feasibility of carbon footprint inventory based on carbon thermal map.

### 5.2 Carbon exergy ratio analysis

The experimental platform took lignite as fuel and was equipped with two 350,000 kw tower-type lignite boiler generator units. Because the example power enterprise is directly connected to the local power grid, there is no energy input in the form of steam or heat, so it's determined that for this power enterprise, the carbide within the plant area has been taken as the boundary. The GHGs of the power enterprise coming from fixed combustion emissions, mobile combustion emissions, processing emissions, and escaped emission sources were identified one by one, and the diagram of boundary identification is shown in Figure 6.

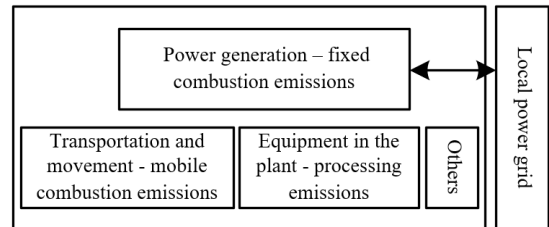


Figure 6. Diagram of boundary identification

Taking the black box model as an example, during boiler operation, the black box model simultaneously undergoes several processes including the combustion of fuel, the heating of water, the transferring of heat from flue gas to water, and the vaporization. From Figure 7, we can get the exergy efficiency of the boiler  $\zeta$ , namely the ratio of exergy gains to exergy loss, and the experimental results showed that, the exergy loss is caused by the irreversibility of combustion and heat transfer in the boiler, and it accounts for more than 60% of the total input exergy. According to Formulas 17 and 18, when the carbon content in the fuel is relatively high, the amount of carbon emission is greater and there is  $\varepsilon < \eta$ , which means that the fuel cannot control the emission of carbides, and burning too much fuel will generate excessive carbon emissions, thereby polluting the ecological environment. According to the carbon exergy process shown in Formula 17,

it can be attained that the exergy emitted by unit fuel in equipment unit 1 is greater than that in equipment unit 2, indicating that under the same conditions, the carbon released from unit 1 is less than that from unit 2.

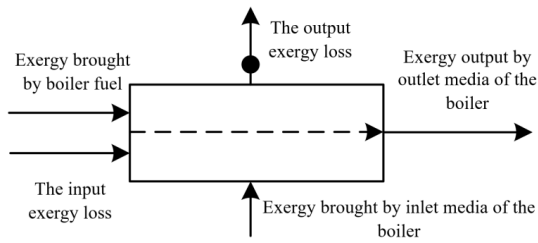


Figure 7. The black box model of boiler exergy balance

### 5.3 Comparative analysis of carbon emissions of the power industry

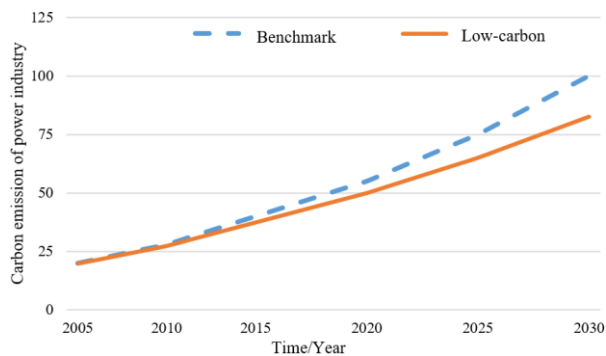


Figure 8. Comparison of carbon emissions of the power industry

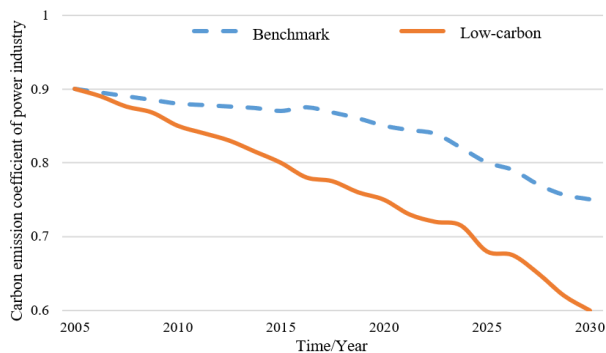


Figure 9. Comparison of carbon emission coefficient of power industry

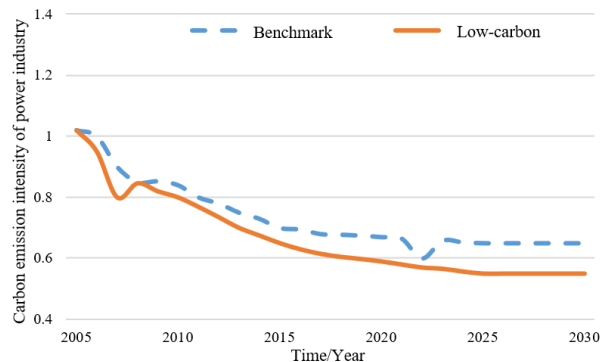


Figure 10. Comparison of carbon emission intensity of power industry

In this paper, two simulation scenarios are assumed, the benchmark scenario, and the low-carbon scenario, then the carbon emission amount, the emission coefficient, and the emission intensity of the power enterprise under these two scenarios are compared and analyzed.

The amount of carbon emissions of the power industry is shown in Figure 8. According to the results of comparative analysis, the emission of the low-carbon scenario is lower than that of the benchmark scenario. Before 2030, carbon emissions will increase due to the following reasons: (1) the non-stop advancement of science and technology will reduce power loss and increase the emission efficiency of power enterprises, thereby directly or indirectly reducing carbon emissions; (2) The power generation structure of the power industry has been developed and innovated constantly, which has effectively realized the low-carbon power transformation of nuclear power, biomass, renewable energy, hydropower, and geothermal power, as a result, the proportion of coal-fired power generation has been greatly reduced.

The carbon emission coefficient of the power industry is shown in Figure 9. Before 2030, the carbon emission coefficient of the power industry will decrease year by year. The emission coefficient under the benchmark scenario is greater than that under the low-carbon scenario, and the difference in the emission coefficient will become larger with the passing of time. At the same time, by 2030, the carbon emission of power industry under low-carbon scenario is expected to be reduced by about 100 million tons compared to that under the benchmark scenario. Under the benchmark scenario, the carbon emission coefficient of the power industry is expected to drop from 0.90 kg/kwh in 2005 to 0.75 kg/kwh in 2030. Under the low-carbon scenario, the carbon emission coefficient of the power industry which exhibits as wave lines is expected to drop from 0.90kg/kwh in 2005 to 0.60 kg/kwh in 2030. The experimental results showed that with the optimization of the power supply structure and the investment in science and technology, the energy utilization rate of the power industry will be improved and the goals of energy conservation, emission reduction, and peak carbon emissions will be realized. After 2030, the carbon emissions of the power industry will continue to decrease, causing the emission coefficient to decline with it.

The carbon emission intensity of the power industry is shown in Figure 10. Under both the benchmark scenario and the low-carbon scenario, the carbon emission intensity of the power industry in China will slowly decrease in the future, and the emission intensity of the benchmark scenario is still higher than that of the low-carbon scenario. There are three reasons for this: (1) As the population is still growing in China, the large population size will inevitably lead to a high demand for electricity, which can make the carbon emissions of power industry to increase, and the emission coefficient and emission intensity decline accordingly; (2) The rapid development of the economy promotes the GDP of the domestic power industry to increase year by year, which has greatly increased the total energy consumption of power enterprises; (3) The improvement of the material living standards of Chinese residents will increase the use frequency of various power facilities and high-tech electrical devices. All the above factors can contribute to the increase of electricity demand and carbon emission, thereby decreasing the carbon emission intensity year by year.

## 5.4 Analysis of inventory results

After simulation analysis, it is attained that the average annual carbide emission of the sample power enterprise during carbon inventory is  $4.55 \text{ MtCO}_2/\text{yr}$ , this data can be taken as the benchmark of the carbon inventory database to carry out the energy conservation and emission reduction works. In this paper, three kinds of data sources are set, namely the heat supply data based on boiler gas supply, the data based on power production, and the data based on fuel supply; by applying different data sources, different inventory results would be attained, and the emission data is shown in Table 3.

**Table 3.** Emission data of boiler combustion

Unit: $\text{MtCO}_2/\text{yr}$	Unit 1	Unit 2
Data based on boiler gas supply	1.75	1.83
Data based on power production	2.03	2.39
Data based on fuel supply	2.25	2.47

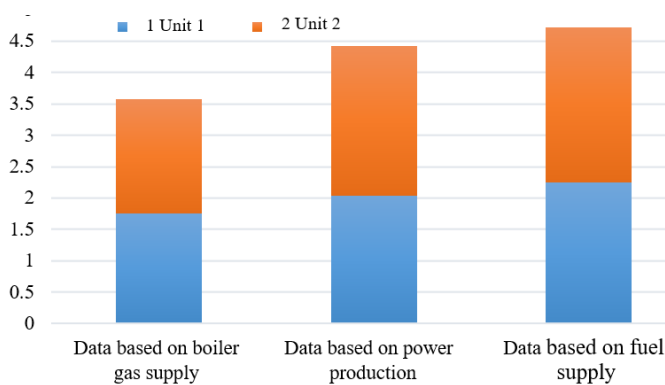


**Figure 11.** Comparison of emission data of fixed combustion of boiler

Because the boiler gas supply data adopted the data of the steam discharged from boiler outlet, and the fuel supply data was attained by converting the carbon content before the fuel enters the boiler, the comparison of the emission data of the fixed combustion of the boiler is shown in Figure 11. For the two types of data sources, the incomplete combustion of carbides would generate different amounts of GHG emissions, and this will lead to differences in the carbon inventory results. Therefore, the boiler gas supply data and the power production data are smaller than the fuel supply data. However, during the calculation process of boiler gas supply data and power production data, a same heat emission factor  $\bar{y}_k$  has been adopted, so the power production data is smaller compared to the fuel supply data, and this means that the energy power provided by the tower-type lignite boiler generator units is less than the energy consumed by power production.

## 6. CONCLUSION

To create low carbon environment and optimize and coordinate the carbon market, in this paper, a carbon footprint tracking and quantitative analysis model for power industry was constructed based on thermodynamics. This paper plotted carbon thermal maps, built a complete carbon inventory system, selected time periods with high efficiency to do the inventory work, and repaired the power enterprises with a carbon emission exceeding the fixed cap at a speed of R. The

repair method is to convert the GHGs into other energy forms or hold them temporarily. The inventory batches are numbered using intervals, which has greatly saved the inventory costs. According to the theory of thermal economics, based on five first-level indexes of carbon exergy ratio, regulatory index, input, output, and environmental variables, this paper further divides them into 10 second-level indexes, their roles are clearly divided and together constitute the complete index system. Under the interactive action of these indexes, the error range of carbon emission intensity could be reduced gradually to facilitate the real-time monitoring of carbon asset information. For enterprises whose emission exceeds the cap, fines or taxes will be imposed on them, while for those who can abide by the contract, carbon quotas will be rewarded to them to improve their credibility. By assessing the dynamic carbon footprint using carbon thermal maps from four dimensions, carbon emissions could be control effectively, in this way, great contributions could be made to the optimization of the ecological environment.

## ACKNOWLEDGEMENT

This paper was supported by Project Supported by National Social Science Fund (Grant No.: 19BGL003).

## REFERENCES

- [1] Wang, J., Jia, C.S., Li, C.J., Peng, X.L., Zhang, L.H., Liu, J.Y. (2019). Thermodynamic properties for carbon dioxide. *ACS Omega*, 4(21): 19193-19198. <https://doi.org/10.1021/acsomega.9b02488>
- [2] Kilci, E.N. (2022). Incentives for Sustainability: Relationship Between Renewable Energy Use and Carbon Emissions for Germany and Finland. *Opportunities and Challenges in Sustainability*, 1(1): 29-37. <https://doi.org/10.56578/ocs010104>.
- [3] Müller, L.J., Kästelhön, A., Bringezu, S., et al. (2020). The carbon footprint of the carbon feedstock CO<sub>2</sub>. *Energy & Environmental Science*, 13(9): 2979-2992. <https://doi.org/10.1039/D0EE01530J>
- [4] Babar, M., Bustam, M.A., Ali, A., et al. (2019). Thermodynamic data for cryogenic carbon dioxide capture from natural gas: A review. *Cryogenics*, 102: 85-104. <https://doi.org/10.1016/j.cryogenics.2019.07.004>
- [5] Fenner, A.E., Kibert, C.J., Woo, J. (2018). The carbon footprint of buildings: A review of methodologies and applications. *Renewable and Sustainable Energy Reviews*, 94: 1142-1152. <https://doi.org/10.1016/j.rser.2018.07.012>
- [6] Lenzen, M., Sun, Y.Y., Faturay, F., Ting, Y.P., Geschke, A., Malik, A. (2018). The carbon footprint of global tourism. *Nature Climate Change*, 8(6): 522-528. <https://doi.org/10.1038/s41558-018-0141-x>
- [7] Yañez, P., Sinha, A., Vásquez, M. (2019). Carbon footprint estimation in a university campus: evaluation and insights. *Sustainability*, 12(1): 181. <https://doi.org/10.3390/su12010181>
- [8] Fan, J., Hong, H., Jin, H. (2018). Biomass and coal co-feed power and SNG polygeneration with chemical looping combustion to reduce carbon footprint for sustainable energy development: Process simulation and

- thermodynamic assessment. *Renewable Energy*, 125: 260-269. <https://doi.org/10.1016/j.renene.2018.02.116>
- [9] Brogioli, D., La Mantia, F. (2021). Innovative technologies for energy production from low temperature heat sources: critical literature review and thermodynamic analysis. *Energy & Environmental Science*, 14(3): 1057-1082. <https://doi.org/10.1039/D0EE02795B>
- [10] Xin, T., Xu, C., Liu, Y., Yang, Y. (2021). Thermodynamic analysis of a novel zero carbon emission coal-based polygeneration system incorporating methanol synthesis and Allam power cycle. *Energy Conversion and Management*, 244: 114441. <https://doi.org/10.1016/j.enconman.2021.114441>
- [11] Marquardt, T., Bode, A., Kabelac, S. (2020). Hydrogen production by methane decomposition: Analysis of thermodynamic carbon properties and process evaluation. *Energy Conversion and Management*, 221: 113125. <http://dx.doi.org/10.1016/j.enconman.2020.113125>
- [12] Wang, S., Liu, C., Ren, J., Liu, L., Li, Q., Huo, E. (2019). Carbon footprint analysis of organic Rankine cycle system using zeotropic mixtures considering leak of fluid. *Journal of Cleaner Production*, 239: 118095. <https://doi.org/10.1016/j.jclepro.2019.118095>
- [13] Shakhbulatov, D., Arora, A., Dong, Z., Rojas-Cessa, R. (2019). Blockchain implementation for analysis of carbon footprint across food supply chain. In 2019 IEEE International Conference on Blockchain (Blockchain), Atlanta, GA, USA, pp. 546-551. <https://doi.org/10.1109/Blockchain.2019.00079>
- [14] Prieto, G. (2017). Carbon dioxide hydrogenation into higher hydrocarbons and oxygenates: thermodynamic and kinetic bounds and progress with heterogeneous and homogeneous catalysis. *ChemSusChem*, 10(6): 1056-1070. <https://doi.org/10.1002/cssc.201601591>
- [15] Adametz, P., Pöttinger, C., Müller, S., et al. (2017). Thermodynamic evaluation and carbon footprint analysis of the application of hydrogen-based energy-storage systems in residential buildings. *Energy Technology*, 5(3): 495-509. <https://doi.org/10.1002/ente.201600388>
- [16] Jradi, S., Chameeva, T.B., Delhomme, B., Jaegler, A. (2018). Tracking carbon footprint in French vineyards: A DEA performance assessment. *Journal of Cleaner Production*, 192: 43-54. <https://doi.org/10.1016/j.jclepro.2018.04.216>
- [17] Jager, H.I., Griffiths, N.A., Hansen, C.H., King, A.W., Matson, P.G., Singh, D., Pilla, R.M. (2022). Getting lost tracking the carbon footprint of hydropower. *Renewable and Sustainable Energy Reviews*, 162: 112408. <http://dx.doi.org/10.1016/j.rser.2022.112408>
- [18] Gao, T., Jin, P., Song, D., Chen, B. (2022). Tracking the carbon footprint of China's coal-fired power system. *Resources, Conservation and Recycling*, 177: 105964. <http://dx.doi.org/10.1016/j.resconrec.2021.105964>
- [19] Gao, D., Joseph, J., Werner, R.A., et al. (2021). Drought alters the carbon footprint of trees in soils-tracking the spatio-temporal fate of <sup>13</sup>C-labelled assimilates in the soil of an old-growth pine forest. *Global Change Biology*, 27(11): 2491-2506. <https://doi.org/10.1111/gcb.15557>